

## I. INTRODUCTION

The Targeting Resources through Exploration and Knowledge project is a multidisciplinary project aimed at bringing together a variety of datasets in order to improve our understanding of the geological framework and mineral potential of the Interior Plateau. In particular, little is known about the structural framework of this region. This region encompasses southern Stikine terrane, Cache Creek terrane, Cadwallader terrane, and several metamorphic complexes (Figure 1). These are extensively mantled by volcanosedimentary overlap assemblages and thick glacial till. Publicly available aeromagnetic and gravity data have been integrated with bedrock mapping to develop a structural framework for the northern Interior Plateau. This new framework outlines several major faults that were previously unidentified. These faults, in part, controlled the development and inversion of the marine Nechako Basin.

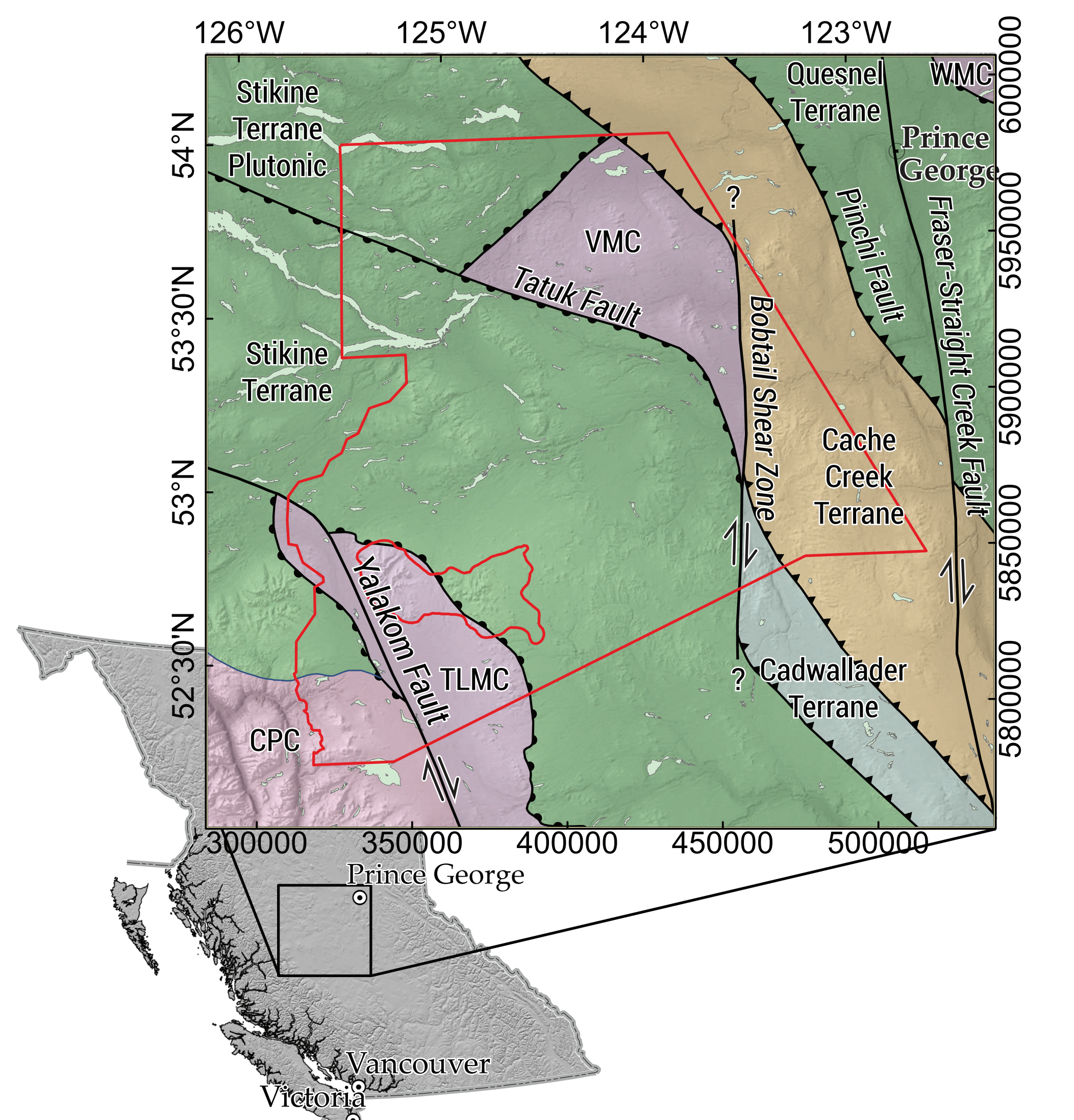


Figure 1: Location of the study area with tectonic domains and major structures based on a combination of British Columbia map compilation, airborne magnetic and gravity data. Some of the structures presented here have not previously been documented. The red line corresponds to the extent of the TREK aeromagnetic survey. TLMC - Tatla Lake Metamorphic Complex, VMC - Vanderhoof Metamorphic Complex, WMC - Wolverine Metamorphic Complex, CPC - Coast Plutonic Complex.

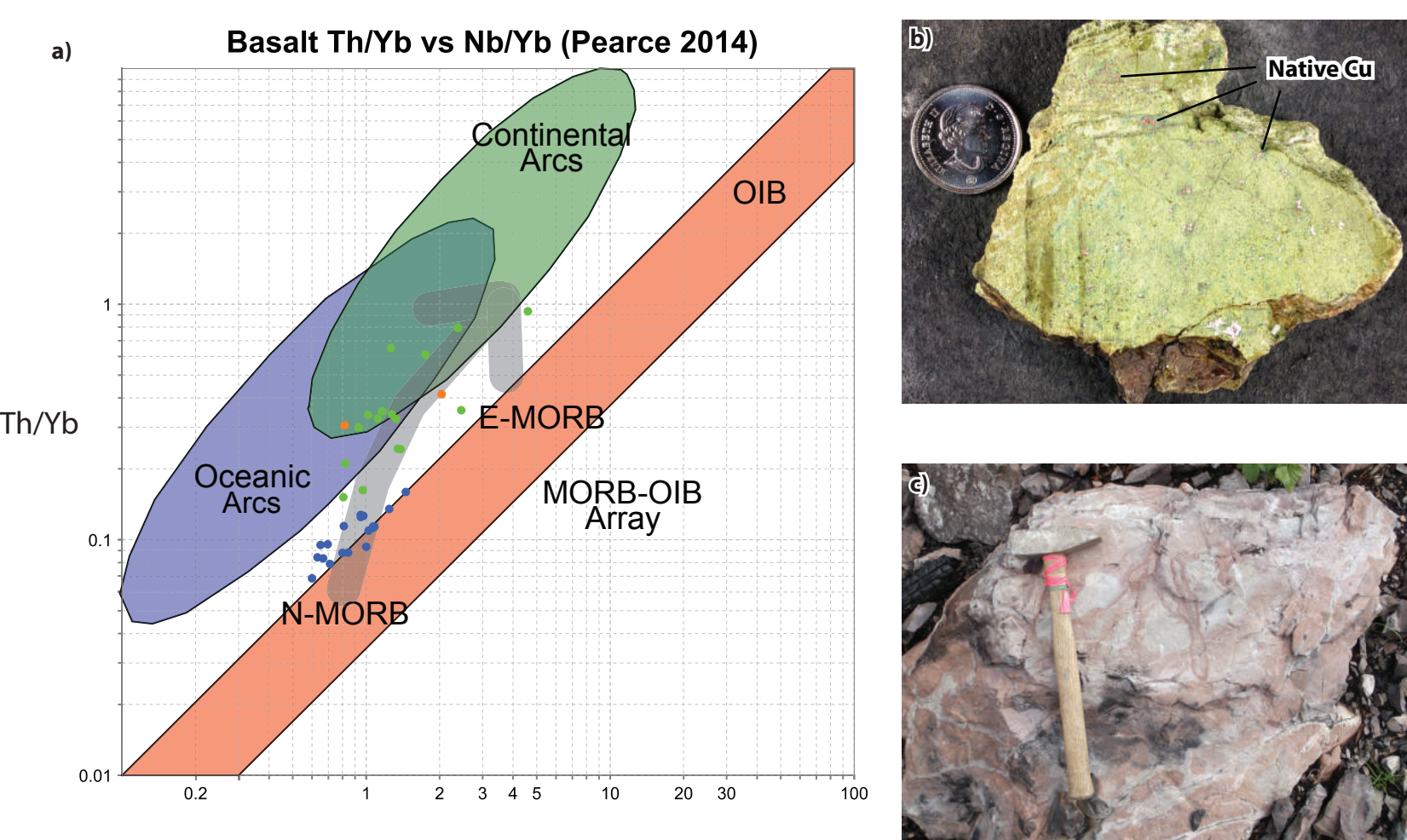


Figure 3: Characteristics of the Liesegang Basalt Unit and associated Volcanic Redbed Cu mineralization: a) Th-Nb proxy of Pearce (2006; 2014). Liesegang Basalt samples plotted in orange. Group 1 and 2 basalts of the IRF are plotted in blue and green respectively. Grey arrow shows contamination trend towards average IRF rhyolite (modified after Barresi et al., 2015); b) Native Cu within an epidote, quartz, calcite vein at the Liesegang showing. This sample yielded >1% Cu and 7.05 g/t Ag; c) Intense Liesegang rings developed in basalt.

## III. MIDDLE JURASSIC DEFORMATION

The newly identified **Tatuk Fault** (Figure 2a) was defined by strong parallel aeromagnetic and gravity anomalies (Figure 2b,c). It marks the northeastern limit of Bowser Lake Group marine strata. When combined with the northeastward thickening of the Bowser Lake Group, this suggests that the Tatuk Fault was present as a basin bounding fault at least by the Middle Jurassic.

The newly identified **Bobtail Shear Zone** (Figure 2a) is represented by a linear aeromagnetic low which juxtaposes distinct domains (Figure 2b). It corresponds to intensely deformed mylonite and gneiss (Figure 4a). Structural measurements include steep foliation and shallow stretching lineations (Figure 4b), consistent with strike slip shear.

It is postulated that normal shear on the Tatuk Fault and sinistral shear on the Bobtail Shear Zone may be coeval as they are both consistent with northeast-southwest directed extension.

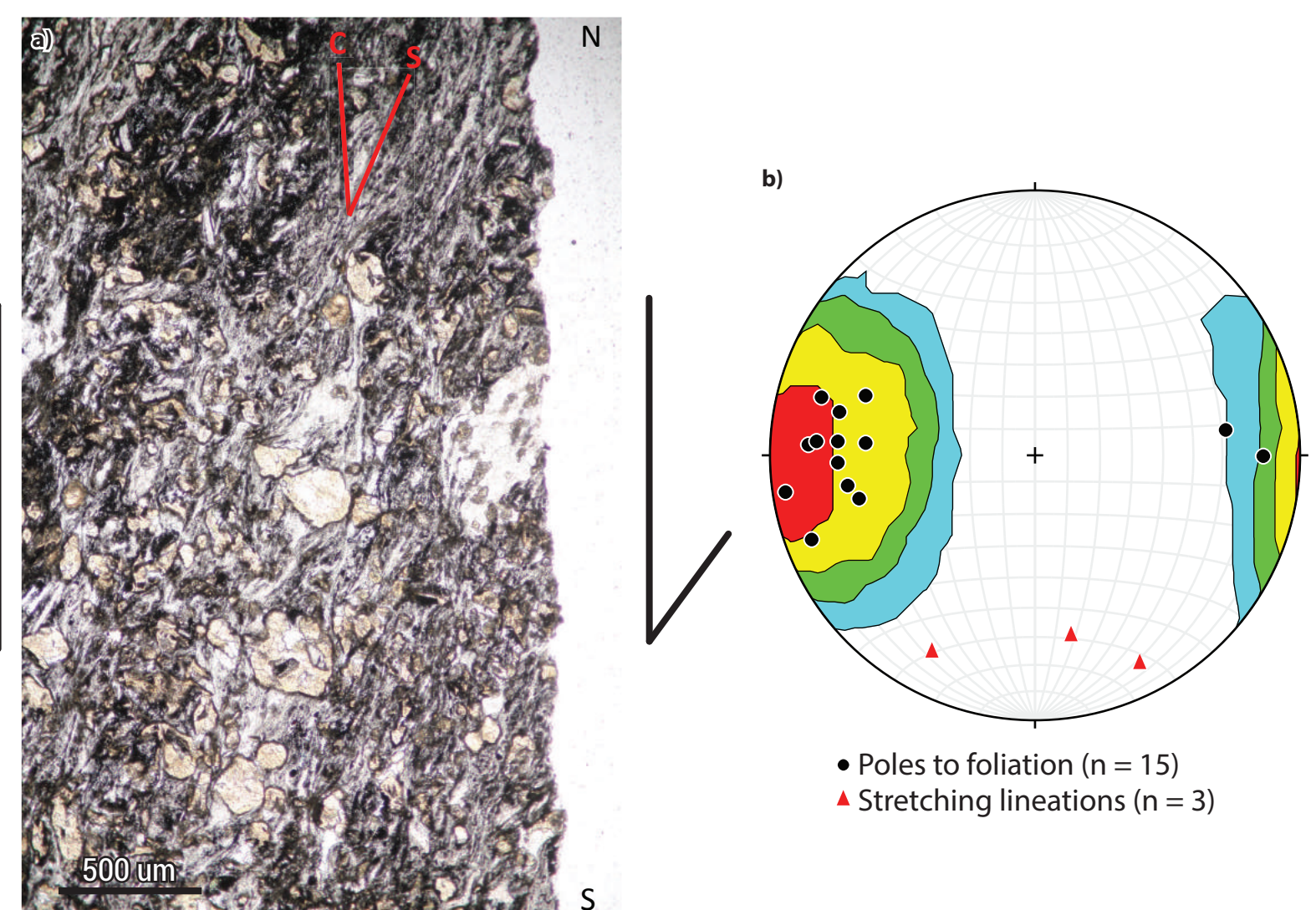


Figure 4: Characteristics of the Bobtail Shear Zone: a) Plane polarized light photomicrograph exhibiting s-c fabric indicative of north-striking sinistral shear; b) Stereonet showing structural measurements consistent with strike-slip shear.

## II. JURASSIC STRATIGRAPHY AND MINERALIZATION

The upper Hazelton Group volcanosedimentary sequence is locally comprised of the Entiako and Naglico formations (Diakow et al., 1997). The stratigraphically lowest of three new units identified at the base of the Entiako Formation, the Liesegang Basalt Unit (Figure 2a) exhibits geochemical similarities to the crustally contaminated rift related basalts of the Iskut River Formation (IRF) (Type 2 of Barresi et al., 2015; Figure 3a). It hosts volcanic redbed Cu mineralization at the new Liesegang and Pickle showings (Figure 2a, 3b). The ubiquitous presence of Liesegang rings in this new basalt unit but not in the younger Naglico Formation or Nechako volcanics suggests that a large hydrothermal system was active shortly after deposition.

The Hazelton Group is conformably overlain by chert rich siliciclastic rocks of the Bowser Lake Group. This group includes a northeastward thickening wedge of coarse clastic rocks, potentially up to 1500 m thick in the northern Nechako Range (Diakow et al., 1997).

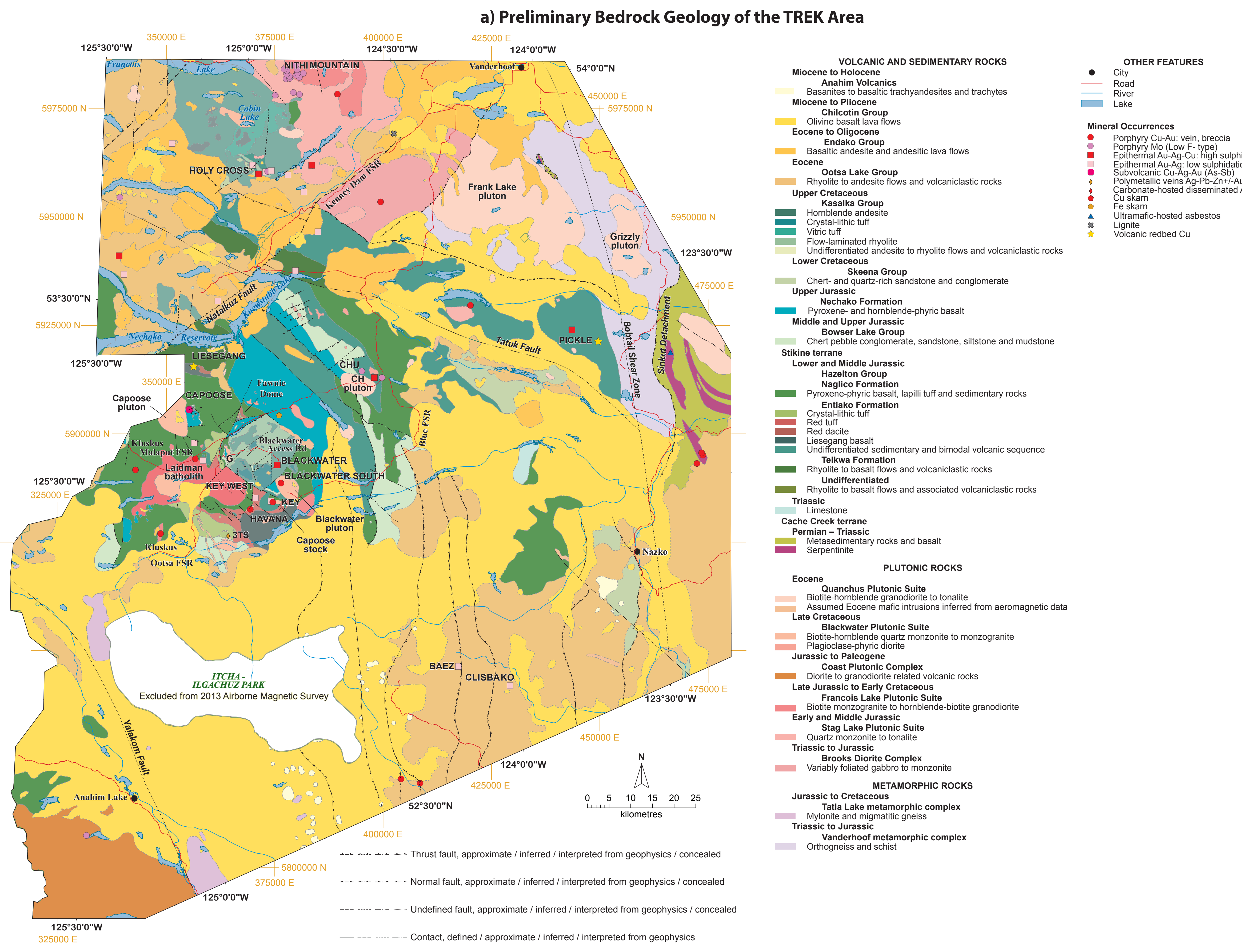


Figure 2: a) Bedrock geology map of the TREK area developed from physical interpretation, targeted bedrock mapping, and compilation of previous mapping including Tipper, 1959, 1963, 1969; Diakow and Levson, 1997; Struik et al., 2007; and Bordet, 2014; b) Reduced to pole magnetic intensity with faults as dashed black lines and folds as dashed white lines (modified after Buckingham, 2014b); c) Isostatic residual gravity response, faults and folds represented as above (modified after Buckingham, 2014b). All maps were produced in NAD 83 BC Environment Albers Projection.

## IV. CRETACEOUS DEFORMATION

The Jurassic strata south of the Tatuk Fault were deformed during ENE- and WSW-vergent fold and thrust deformation (Figure 5a). This is likely related to the 700 km long fold and thrust belt that flanks the east side of the Coast Belt (Rusmore and Woodsworth, 1991; Evenchick et al., 1991; Schiarizza et al., 1997; Rusmore et al., 2000). Field structural evidence and geophysical anomalies exhibit a curvature from NNW-SSE to WNW-ESE with proximity to the Tatuk Fault (Figure 2; Figure 3b,c). The predominantly volcanic and plutonic rocks to the north of the Tatuk Fault appear unaffected by the mid-Cretaceous deformation so it behaved as a sinistral fault to accommodate the shortening within the basin. The Nazko-Redstone belt, along the eastern margin of this fold and thrust belt, is interpreted to have formed similar to the Sustut Basin to the north. Deformation continued at least until the Campanian as indicated by palynology of well logs showing Albion to Cenomanian strata on top of Campanian strata (Riddell, 2011).

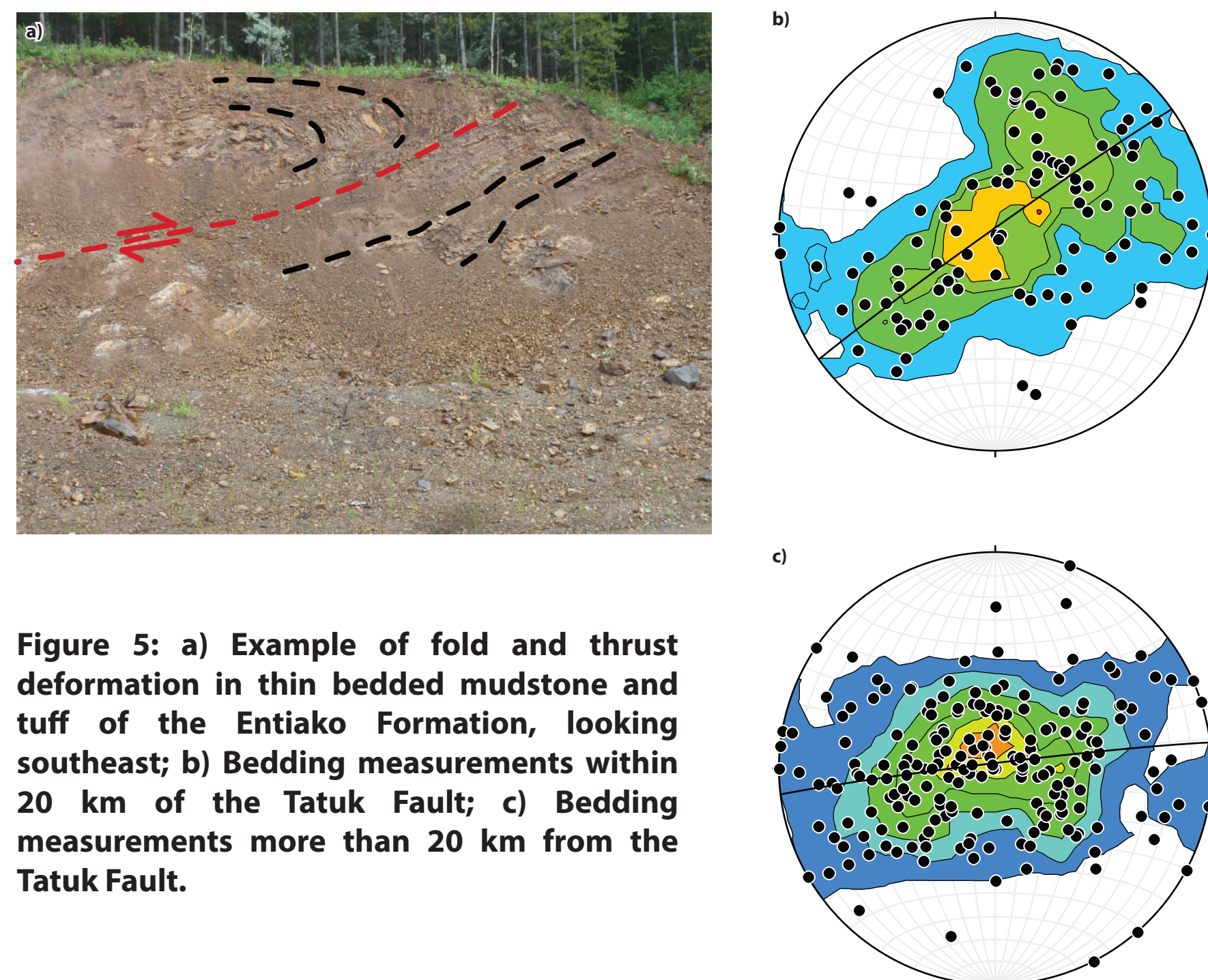


Figure 5: a) Example of fold and thrust deformation in thin bedded mudstone and tuff of the Entiako Formation, looking southeast; b) Bedding measurements within 20 km of the Tatuk Fault; c) Bedding measurements more than 20 km from the Tatuk Fault.

## V. EOCENE DEFORMATION

Eocene deformation was characterized by extension that can be separated into two phases. The early phase of nearly E-W extension is recorded by NW-SE striking dextral faults, including reactivation of the Tatuk Fault, and N-S striking normal faults, including reactivation of some mid-Cretaceous thrust faults (Bordet, 2014). It accompanied eruption of the Ootsa Lake Group (Bordet, 2014) and exhumation of the Tatla Lake Metamorphic Complex (Friedman and Armstrong, 1988). The late phase represents NW-SE extension recorded by N-S striking dextral faults, NE-SW striking normal faults, and exhumation of the Vanderhoof Metamorphic Complex along the Sinkut Detachment (Figure 2a; Wetherup and Struik, 1996). It is assumed that the Bobtail Shear Zone accommodated some amount of dextral shear at this time given the current juxtaposition of geological units and its orientation parallel to other late Eocene dextral faults. Eruption of the Endako Group accompanied development of this later phase of extensional deformation, with the Nataukuz Fault locally forming a boundary for the basalt (Figure 2a). The Endako Group geochemistry shows evidence for melting of an enriched mantle source, consistent with an extensional setting (Figure 6).

## VII. DISCUSSION

The presence of a rift related basalt at the base of the upper Hazelton Group suggests that the Jurassic transtension recorded by the Tatuk Fault and Bobtail Shear Zone may have initiated in the Early Jurassic. This is in agreement with a proposed Early Jurassic transtensional origin for the Bowser Basin to the north (Greig et al., 1991). A sinistral component to convergence is supported by relative plate motion models (Engelbreton et al., 1985), and by paleomagnetic results (McCaulland, 2006). Similarly oriented structures bounding the Bowser Basin in the Spatsizi River area documented by Evenchick and Thorkelson (1995) may have a shared Early to Middle Jurassic history.

## IX. CONCLUSIONS

The Tatuk Fault is a cryptic southeast striking normal fault that formed the northeastern margin of the Nechako basin in the latest Middle Jurassic. It may be cogenetic with the north striking sinistral Bobtail Shear Zone, consistent with NE-SW directed extension, or overall sinistral transtension. The newly identified Liesegang basalt unit which hosts native Cu mineralization may be genetically related to initial opening of the Nechako basin. The Tatuk Fault is a major structural break that was reactivated during mid-Cretaceous compression Eocene extension.

## REFERENCES:

Barresi, T., Nelson, J.L., and Dostal, J. (2015). Geochemical constraints on magmatic and metamorphic processes: Iskut River Formation, volcanogenic massive sulfide-hosting basalts, NW British Columbia, Canada. *Canadian Journal of Earth Sciences*, v. 52, p. 1-20.  
Bordet, E. (2014). Eocene volcanic response to the tectonic evolution of the Canadian Cordillera. Ph.D. thesis, University of British Columbia, 220 p.  
Buckingham, A. (2014a). Enhancement filtering and structural detection, magnetic data, MDRU TREK project, unpublished report, Fathom Geophysics, August 2014, 22p.  
Buckingham, A. (2014b). Enhancement filtering and structural detection, gravity data, MDRU TREK project, unpublished report, Fathom Geophysics, August 2014, 22p.  
Diakow, L.J., and Levson, I.M. (1997). Bedrock and surface geology of the southern Nechako plateau, central British Columbia, BC Ministry of Energy and Mines, BC Geological Survey, Geoscience Map 1697-2, scale 1:100 000.  
Diakow, L.J., Webster, C.L., Richards, T.A., and Tipper, H.W. (1997). Geology of the Fawnie and Nechako ranges, southern Nechako Plateau, central British Columbia (53°2' S, 6° 7'), in *Interior Plateau Geoscience Project: Summary of Geological, Geomorphological and Geophysical Studies*, L.J. Diakow, J.M. Newell and J. Metcalfe (ed.), BC Ministry of Energy and Mines, BC Geological Survey, Open File 1697-2 and Geological Survey of Canada, Open File 3448, p. 1-30.  
Engelbreton, D.C., Cox, A., Gordon, R.G. (1985). Relative Motions between Oceanic and Continental Plates in the Pacific Basin. *Geological Society of America, Special Paper* 206, p. 1-59.  
Evenchick, C.A. (1991). Geometry, evolution, and tectonic framework of the Skeena Fold Belt, North Central British Columbia, *Tectonics*, v. 10, p. 527-546.  
Evenchick, C.A., and Thorkelson, D.J. (2005). Geology of the Spatsizi River map area, north-central British Columbia. *Geological Survey of Canada Bulletin* 577, p. 278.  
Greig, C.J., Gehrels, G.E., Anderson, R.O., Evenchick, C.A. (1991). Possible transpressional origin of the Bowser Basin, British Columbia. In: *Geological Society of America, Abstract with Programs*, vol. 23, p. 30. Pearce, J.A. (2009). Geochemical interpretation of oceanic basalts with applications to ophiolite classification and the search for Archean oceanic crust. *Lithos*, v. 100, p. 14-48.  
McCaulland, P.J.A., Symon, D.T.A., Hart, C.J.R., and Blackburn, W.H. (2005). Assembly of the northern Cordillera: New paleomagnetic evidence for coherent, moderate Jurassic to Eocene motion of the Intermontane belt and Yukon-Tanana terranes. In: Haggart, J.W., Erkin, R.J., and Monger, J.W.H. eds. *Paleogeography of the North American Cordillera: Evidence For and Against Large-Scale Displacements*, Geological Association of Canada, Special Paper 46, p. 147-170.  
Pearce, J.A. (2014). Immobility element fingerprinting of ophiolites. *Elements*, v. 10, p. 101-108.  
Rusmore, M.E., and Woodsworth, G.L. (1991). Coast Plutonic Complex: A mid-Cretaceous contractional orogen. *Geology*, v. 19, p. 941-944.  
Rusmore, M.E., Woodsworth, G.L., and Gehrels, G.E. (2000). Late Cretaceous evolution of the eastern Coast Mountains, British Columbia, in: *Tectonics of the Coast Mountains, southeastern Alaska and British Columbia*, edited by H.H. Stewart and W.C. McClelland. *Geological Society of America, Special Paper*, v. 343, p. 89-105.  
Schiarizza, P., Gaba, R.G., Glover, J.K., Gower, J.I., and Linnhorst, J.P. (1997). Geology and mineral occurrences of the Taseko - Bridge River area, B.C. Ministry of Employment and Investment, Energy and Minerals Division, *Geological Survey Branch Bulletin* 100, 222 p.  
Struik, L.C., MacIntyre, D.C., and Williams, S.P. (2007). Nechako NATMAP Project: A Digital Suite of Geoscience Information for Central British Columbia/NTS Map Sheets 093N, 093K, 093P, 093G, 093L, 093M, 093N, 093P, 093Q, 093R, 093S, 093T, 093U, 093V, 093W, 093X, 093Y, 093Z, 093AA, 093AB, 093AC, 093AD, 093AE, 093AF, 093AG, 093AH, 093AI, 093AJ, 093AK, 093AL, 093AM, 093AN, 093AO, 093AP, 093AQ, 093AR, 093AS, 093AT, 093AU, 093AV, 093AW, 093AX, 093AY, 093AZ, 093BA, 093BB, 093BC, 093BD, 093BE, 093BF, 093BG, 093BH, 093BI, 093BJ, 093BK, 093BL, 093BM, 093BN, 093BO, 093BP, 093BQ, 093BR, 093BS, 093BT, 093BU, 093BV, 093BW, 093BX, 093BY, 093BZ, 093CA, 093CB, 093CC, 093CD, 093CE, 093CF, 093CG, 093CH, 093CI, 093CJ, 093CK, 093CL, 093CM, 093CN, 093CO, 093CP, 093CQ, 093CR, 093CS, 093CT, 093CU, 093CV, 093CW, 093CX, 093CY, 093CZ, 093DA, 093DB, 093DC, 093DD, 093DE, 093DF, 093DG, 093DH, 093DI, 093DJ, 093DK, 093DL, 093DM, 093DN, 093DO, 093DP, 093DQ, 093DR, 093DS, 093DT, 093DU, 093DV, 093DW, 093DX, 093DY, 093DZ, 093EA, 093EB, 093EC, 093ED, 093EE, 093EF, 093EG, 093EH, 093EI, 093EJ, 093EK, 093EL, 093EM, 093EN, 093EO, 093EP, 093EQ, 093ER, 093ES, 093ET, 093EU, 093EV, 093EW, 093EX, 093EY, 093EZ, 093FA, 093FB, 093FC, 093FD, 093FE, 093FF, 093FG, 093FH, 093FI, 093FJ, 093FK, 093FL, 093FM, 093FN, 093FO, 093FP, 093FQ, 093FR, 093FS, 093FT, 093FU, 093FV, 093FW, 093FX, 093FY, 093FZ, 093GA, 093GB, 093GC, 093GD, 093GE, 093GF, 093GG, 093GH, 093GI, 093GJ, 093GK, 093GL, 093GM, 093GN, 093GO, 093GP, 093GQ, 093GR, 093GS, 093GT, 093GU, 093GV, 093GW, 093GX, 093GY, 093GZ, 093HA, 093HB, 093HC, 093HD, 093HE, 093HF, 093HG, 093HH, 093HI, 093HJ, 093HK, 093HL, 093HM, 093HN, 093HO, 093HP, 093HQ, 093HR, 093HS, 093HT, 093HU, 093HV, 093HW, 093HX, 093HY, 093HZ, 093IA, 093IB, 093IC, 093ID, 093IE, 093IF, 093IG, 093IH, 093II, 093IJ, 093IK, 093IL, 093IM, 093IN, 093IO, 093IP, 093IQ, 093IR, 093IS, 093IT, 093IU, 093IV, 093IW, 093IX, 093IY, 093IZ, 093JA, 093JB, 093JC, 093JD, 093JE, 093JF, 093JG, 093JH, 093JI, 093JJ, 093JK, 093JL, 093JM, 093JN, 093JO, 093JP, 093JQ, 093JR, 093JS, 093JT, 093JU, 093JV, 093JW, 093JX, 093JY, 093JZ, 093KA, 093KB, 093KC, 093KD, 093KE, 093KF, 093KG, 093KH, 093KI, 093KJ, 093KL, 093KM, 093KN, 093KO, 093KP, 093KQ, 093KR, 093KS, 093KT, 093KU, 093KV, 093KW, 093KX, 093KY, 093KZ, 093LA, 093LB, 093LC, 093LD, 093LE, 093LF, 093LG, 093LH, 093LI, 093LJ, 093LK, 093LL, 093LM, 093LN, 093LO, 093LP, 093LQ, 093LR, 093LS, 093LT, 093LU, 093LV, 093LW, 093LX, 093LY, 093LZ, 093MA, 093MB, 093MC, 093MD, 093ME, 093MF, 093MG, 093MH, 093MI, 093MJ, 093MK, 093ML, 093MN, 093MO, 093MP, 093MQ, 093MR, 093MS, 093MT, 093MU, 093MV, 093MW, 093MX, 093MY, 093MZ, 093NA, 093NB, 093NC, 093ND, 093NE, 093NF, 093NG, 093NH, 093NI, 093NJ, 093NK, 093NL, 093NM, 093NO, 093NP, 093NQ, 093NR, 093NS, 093NT, 093NU, 093NV, 093NW, 093NX, 093NY, 093NZ, 093OA, 093OB, 093OC, 093OD, 093OE, 093OF, 093OG, 093OH, 093OI, 093OJ, 093OK, 093OL, 093OM, 093ON, 093OO, 093OP, 093OQ, 093OR, 093OS, 093OT, 093OU, 093OV, 093OW, 093OX, 093OY, 093OZ, 093PA, 093PB, 093PC, 093PD, 093PE, 093PF, 093PG, 093PH, 093PI, 093PJ, 093PK, 093PL, 093PM, 093PN, 093PO, 093PP, 093PQ, 093PR, 093PS, 093PT, 093PU, 093PV, 093PW, 093PX, 093PY, 093PZ, 093QA, 093QB, 093QC, 093QD, 093QE, 093QF, 093QG, 093QH, 093QI, 093QJ, 093QK, 093QL, 093QM, 093QN, 093QO, 093QP, 093QQ, 093QR, 093QS, 093QT, 093QU, 093QV, 093QW, 093QX, 093QY, 093QZ, 093RA, 093RB, 093RC, 093RD, 093RE, 093RF, 093RG, 093RH, 093RI, 093RJ, 093RK, 093RL, 093RM, 093RN, 093RO, 093RP, 093RQ, 093RR, 093RS, 093RT, 093RU, 093RV, 093RW, 093RX, 093RY, 093RZ, 093SA, 093SB, 093SC, 093SD, 093SE, 093SF, 093SG, 093SH, 093SI, 093SJ, 093SK, 093SL, 093SM, 093SN, 093SO, 093SP, 093SQ, 093SR, 093SS, 093ST, 093SU, 093SV, 093SW, 093SX, 093SY, 093SZ, 093TA, 093TB, 093TC, 093TD, 093TE, 093TF, 093TG, 093TH, 093TI, 093TJ, 093TK, 093TL, 093TM, 093TN, 093TO, 093TP, 093TQ, 093TR, 093TS, 093TT, 093TU, 093TV, 093TW, 093TX, 093TY, 093TZ, 093UA, 093UB, 093UC, 093UD, 093UE, 093UF, 093UG, 093UH, 093UI, 093UJ, 093UK, 093UL, 093UM, 093UN, 093UO, 093UP, 093UQ, 093UR, 093US, 093UT, 093UU, 093UV, 093UW, 093UX, 093UY, 093UZ, 093VA, 093VB, 093VC, 093VD, 093VE, 093VF, 093VG, 093VH, 093VI, 093VJ, 093VK, 093VL, 093VM, 093VN, 093VO, 093VP, 093VQ, 093VR, 093VS, 093VT, 093VU, 093VV, 093VW, 093VX, 093VY, 093VZ, 093WA, 093WB, 093WC, 093WD, 093WE, 093WF, 093WG, 093WH, 093WI, 093WJ, 093WK, 093WL, 093WM, 093WN, 093WO, 093WP, 093WQ, 093WR, 093WS, 093WT, 093WU, 093WV, 093WW, 093WX, 093WY, 093WZ, 093XA, 093XB, 093XC, 093XD, 093XE, 093XF, 093XG, 093XH, 093XI, 093XJ, 093XK, 093XL, 093XM, 093XN, 093XO, 093XP, 093XQ, 093XR, 093XS, 093XT, 093XU, 093XV, 093XW, 093XX, 093XY, 093XZ, 093YA, 093YB, 093YC, 093YD, 093YE, 093YF, 093YG, 093YH, 093YI, 093YJ, 093YK, 093YL, 093YM, 093YN, 093YO, 093YP, 093YQ, 093YR, 093YS, 093YT, 093YU, 093YV, 093YW, 093YX, 093YY, 093YZ, 093ZA, 093ZB, 093ZC, 093ZD, 093ZE, 093ZF, 093ZG, 093ZH, 093ZI, 093ZJ, 093ZK, 093ZL, 093ZM, 093ZN, 093ZO, 093ZP, 093ZQ, 093ZR, 093ZS, 093ZT, 093ZU, 093ZV, 093ZW, 093ZX, 093ZY, 093ZZ.



For more information, contact:  
Joel Angen, MSc, G.I.T.  
j.angen@eos.ubc.ca